

## LABORATORY INVESTIGATION

## Validating the inspired sinewave technique to measure the volume of the 'baby lung' in a porcine lung-injury model

Douglas C. Crockett<sup>1,\*</sup>, Minh C. Tran<sup>1,2</sup>, Federico Formenti<sup>1,3,4</sup>, John N. Cronin<sup>3</sup>, Göran Hedenstierna<sup>5</sup>, Anders Larsson<sup>6</sup>, Phi A. Phan<sup>1</sup> and Andrew D. Farmery<sup>1</sup>

<sup>1</sup>Nuffield Division of Anaesthetics, University of Oxford, Oxford, UK, <sup>2</sup>Department of Engineering Science, University of Oxford, Oxford, UK, <sup>3</sup>Centre for Human and Applied Physiological Sciences, King's College, London, UK, <sup>4</sup>Department of Biomechanics, University of Nebraska, Omaha, NE, USA, <sup>5</sup>Hedenstierna Laboratory, Department of Medical Sciences, Uppsala University, Uppsala, Sweden and <sup>6</sup>Department of Surgical Sciences, Uppsala University, Uppsala, Sweden

\*Corresponding author. E-mail: [douglas.crockett@ndcn.ox.ac.uk](mailto:douglas.crockett@ndcn.ox.ac.uk)

## Abstract

**Background:** Bedside lung volume measurement could personalise ventilation and reduce driving pressure in patients with acute respiratory distress syndrome (ARDS). We investigated a modified gas-dilution method, the inspired sinewave technique (IST), to measure the effective lung volume (ELV) in pigs with uninjured lungs and in an ARDS model.

**Methods:** Anaesthetised mechanically ventilated pigs were studied before and after surfactant depletion by saline lavage. Changes in PEEP were used to change ELV. Paired measurements of absolute ELV were taken with IST (ELV<sub>IST</sub>) and compared with gold-standard measures (sulphur hexafluoride wash in/washout [ELV<sub>SF6</sub>] and computed tomography (CT) [ELV<sub>CT</sub>]). Measured volumes were used to calculate changes in ELV ( $\Delta$ ELV) between PEEP levels for each method ( $\Delta$ ELV<sub>IST</sub>,  $\Delta$ ELV<sub>SF6</sub>, and  $\Delta$ ELV<sub>CT</sub>).

**Results:** The coefficient of variation was <5% for repeated ELV<sub>IST</sub> measurements ( $n=13$  pigs). There was a strong linear relationship between ELV<sub>IST</sub> and ELV<sub>SF6</sub> in uninjured lungs ( $r^2=0.97$ ), and with both ELV<sub>SF6</sub> and ELV<sub>CT</sub> in the ARDS model ( $r^2=0.87$  and  $0.92$ , respectively). ELV<sub>IST</sub> had a mean bias of  $-12$  to  $13\%$  (95% limits= $\pm 17 - 25\%$ ) compared with ELV<sub>SF6</sub> and ELV<sub>CT</sub>.  $\Delta$ ELV<sub>IST</sub> was concordant with  $\Delta$ ELV<sub>SF6</sub> and  $\Delta$ ELV<sub>CT</sub> in 98–100% of measurements, and had a mean bias of  $-73$  to  $-77$  ml (95% limits= $\pm 128 - 186$  ml) compared with  $\Delta$ ELV<sub>SF6</sub> and  $-1$  ml (95% limits  $\pm 333$  ml) compared with  $\Delta$ ELV<sub>CT</sub>.

**Conclusions:** IST provides a repeatable measure of absolute ELV and shows minimal bias when tracking PEEP-induced changes in lung volume compared with CT in a saline-lavage model of ARDS.

**Keywords:** ARDS; computed tomography; inspired sinewave technique; lung volume measurement; method comparison

## Editor's key points

- The development of lung volume measurements at the bedside may enable personalised ventilatory strategies that optimise respiratory function in acute lung injury.
- The authors used a modified gas-dilution method—the inspired sinewave technique—to measure effective lung volume measured by CT in mechanically

ventilated pigs with uninjured lungs and acute respiratory distress syndrome (ARDS) induced by saline lavage.

- The inspired sinewave technique provided a repeatable measure of absolute effective lung volume.
- This individualised measurement approach may help reduce ventilator-induced injury during ARDS and acute lung injury.

Received: 16 September 2019; Accepted: 16 November 2019

© 2019 The Author(s). Published by Elsevier Ltd on behalf of British Journal of Anaesthesia. This is an open access article under the CC BY license (<http://creativecommons.org/licenses/by/4.0/>).

For Permissions, please email: [permissions@elsevier.com](mailto:permissions@elsevier.com)

The acute respiratory distress syndrome (ARDS) affects 10% of critical care patients and has an associated mortality of 40%.<sup>1</sup> Patients with ARDS have a smaller aerated lung volume ('baby lung') and one of the few interventions shown to reduce mortality in ARDS is ventilating patients with 6–8 ml kg<sup>-1</sup> tidal volume ( $V_T$ ).<sup>2–4</sup> More recently, driving pressure ( $\Delta P$ ) has been shown to be the ventilator parameter that best stratifies risk of mortality in ARDS.<sup>5</sup>  $\Delta P$  is dependent on  $V_T$  and respiratory system compliance ( $C_{RS}$ ) ( $\Delta P = V_T / C_{RS}$ ).  $C_{RS}$  is dependent on the size of the baby lung, and therefore, so too is  $\Delta P$ .<sup>6</sup> It is thought that reduced mortality from low  $V_T$  ventilation may be secondary to reducing the effect that  $\Delta P$  has on the ARDS baby lung.<sup>3</sup>

Whilst it might be possible to titrate  $V_T$  to  $\Delta P$ ,<sup>7</sup> the underlying volume of the baby lung remains the fundamental parameter on which the imposed  $V_T$  exerts its effect to produce  $\Delta P$ . Therefore, there would be potential benefit in measuring the volume of lung of the baby lung at the bedside of a mechanically ventilated ARDS patient. This would allow personalised titration of  $V_T$  to the underlying lung volume, with limitation of lung strain caused by  $\Delta P$ . Lung volume can be measured in ventilated patients by imaging (CT), wash-in/washout techniques, or gas-dilution techniques. CT imaging puts patients at risk by necessitating a transfer to the scanner and exposure to ionising radiation. The current bedside gas-based techniques have not proved reliable in assisted ventilation, or they require equipment that is too bulky or too time-consuming for bedside clinical use.<sup>8–13</sup>

The inspired sinewave technique (IST) has the potential to provide bedside measurement of the lung volume, which takes part in gas exchange (effective lung volume [ELV]). IST uses a low concentration of tracer gas (<5% nitrous oxide [ $N_2O$ ]) injected into the inspired airway gases in a sinusoidally oscillating concentration.<sup>14–16</sup> Sinewave amplitude and phase of the concentration of the tracer gas measured in the expiratory airway gases are used to recover values of ELV ( $ELV_{IST}$ )

and pulmonary blood flow. IST uses commercially available components commonly used in anaesthetic/intensive care practice, and has proven efficacy in spontaneously ventilating healthy volunteers.<sup>17,18</sup> To date, IST's ability to measure ELV in mechanically ventilated lungs has not been tested.

The aim of the current study was to conduct a method comparison, measuring the relationship and limits of agreement between ELV measured by IST compared with SF<sub>6</sub> wash in/washout and CT. To do this, we compared the absolute ELV and changes in ELV ( $\Delta ELV$ ) at and between different PEEPs in mechanically ventilated pigs both before and after induction of ARDS by saline lavage.<sup>10,19,20</sup>

## Methods

### Ethical approval

This study of 13 domestic pigs (mean weight [standard deviation] = 29 [2] kg) at the Hedenstierna Laboratory, Uppsala

**Table 1** Baseline characteristics for  $n=13$  animals pre- and post-lung injury. Mean (standard deviation) are shown for parametric data and median (95% confidence interval) for non-parametric data.  $P$ -values in the final column represent results of either paired Student's  $t$ -test (of parametric data) or Wilcoxon signed rank test (of non-parametric data). CO, cardiac output; DBP, diastolic BP;  $FIO_2$ , fraction of inspired O<sub>2</sub>; Hb, haemoglobin; PaCO<sub>2</sub>, arterial CO<sub>2</sub> partial pressure; PADP, pulmonary artery diastolic BP; PaO<sub>2</sub>, arterial O<sub>2</sub> partial pressure; PASP, pulmonary artery systolic pressure; PFR, PaO<sub>2</sub>:FIO<sub>2</sub> ratio; SaO<sub>2</sub>, arterial oxygen saturation; SBP, systolic BP.

| Parameter                 | Pre-injury       | Post-injury      | $P$ -value |
|---------------------------|------------------|------------------|------------|
| Weight                    | 29 (2)           | —                |            |
| HR (bpm)                  | 86 (70–100)      | 85 (80–95)       | 0.42       |
| SBP (mm Hg)               | 100 (8)          | 98 (14)          | 0.57       |
| DBP (mm Hg)               | 67 (12)          | 54 (8)           | 0.0006     |
| CO (L min <sup>-1</sup> ) | 3.4 (0.8)        | 3.2 (0.4)        | 0.26       |
| PASP (mm Hg)              | 28 (25–33)       | 32 (29–36)       | 0.03       |
| PADP (mm Hg)              | 16 (4)           | 19 (5)           | 0.004      |
| Hb (g dl <sup>-1</sup> )  | 83 (5)           | 84 (6)           | 0.93       |
| $FIO_2$                   | 0.4 (0.3–0.4)    | 0.8 (0.7–0.9)    | 0.0002     |
| SaO <sub>2</sub> (%)      | 100 (99–100)     | 98 (91–99)       | 0.001      |
| pH                        | 7.38 (0.07)      | 7.25 (0.08)      | 0.0004     |
| PaO <sub>2</sub> (kPa)    | 19.2 (15.9–21.5) | 12.8 (11.3–26.0) | 0.39       |
| PaCO <sub>2</sub> (kPa)   | 6.7 (1.1)        | 8.4 (2.0)        | 0.003      |
| PFR                       | 377 (304–513)    | 128 (101–248)    | 0.0002     |

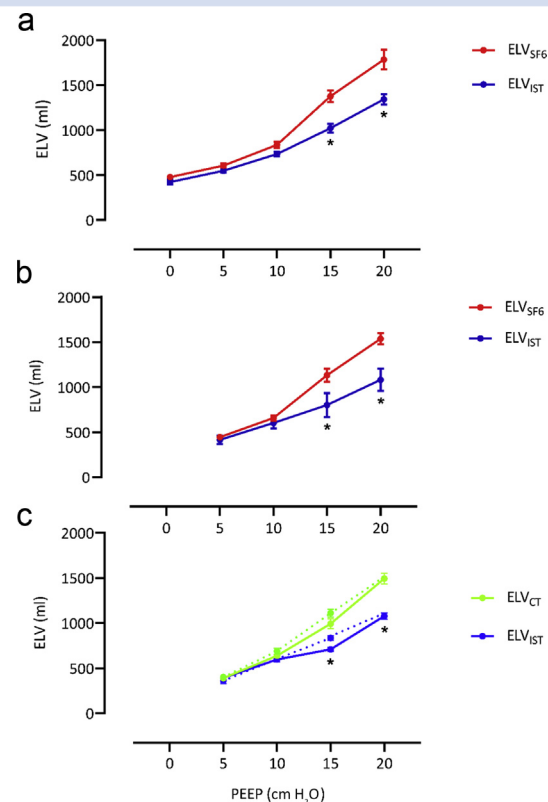


**Fig 1.** Effective lung volume (ELV) measurement (standard error) using  $ELV_{IST}$ ,  $ELV_{SF_6}$ , and  $ELV_{CT}$  at each PEEP level. (a) Paired  $ELV_{IST}$  and  $ELV_{SF_6}$  measurements in the uninjured lung. (b) Paired  $ELV_{IST}$  and  $ELV_{SF_6}$  measurements in the acute respiratory distress syndrome (ARDS) model. (c) Paired  $ELV_{IST}$  and  $ELV_{CT}$  measurements in the ARDS model. PEEP=0 cm H<sub>2</sub>O was not studied post-injury; PEEP levels of 15 and 20 cm H<sub>2</sub>O were studied in six of the total  $n=13$  animals. Solid lines represent volumes measured during incremental PEEP titration; dashed lines represent volumes measured during decremental PEEP titration. \* $ELV_{IST}$  is significantly different to  $ELV_{SF_6}$  or  $ELV_{CT}$  ( $P > 0.05$ ). Table 2 provides full details of volumes measured and probabilities of difference.

University, Uppsala, Sweden was approved by the regional animal welfare and ethics committee (Ref: C98/16). Reporting in this paper adheres to the Animal Research: Reporting of In Vivo Experiments guidelines.<sup>21</sup>

### Animal preparation

Table 1 shows the summary baseline characteristics of the animals pre- and post-lung injury (individual values are given in Supplementary Table 1). The animals were prepared and anaesthetised using i.m. sedation and subsequent i.v. anaesthesia as described elsewhere.<sup>22</sup> During preparation, mechanical ventilation was delivered in volume-controlled ventilation (VCV) mode at 20–25 bpm (to maintain end-tidal CO<sub>2</sub> [EtCO<sub>2</sub>] between 4.5 and 6 kPa), with a V<sub>T</sub> of 10 ml kg<sup>-1</sup>, PEEP of 5 cm H<sub>2</sub>O, and an inspiratory:expiratory ratio (I:E) of 1:2 (Servo-I®; Maquet, Rastatt, Germany). Airway leaks were excluded by analysis of spirometry data. Depth of anaesthesia was confirmed by lack of spontaneous movements, absence of reaction to painful stimulation between the front hooves, and absence of cardiovascular signs of sympathetic stimulation (increases in HR or arterial BP). Subsequent muscle relaxation was achieved with a bolus of rocuronium 0.2 mg kg<sup>-1</sup> followed by 0.1 mg kg<sup>-1</sup> boluses when spontaneous ventilatory efforts were detected from the airway gas and pressure traces. Maintenance i.v. crystalloid fluids were administered (Ringfundin®; B. Braun Melsungen AG, Melsungen, Germany) at a rate of 10 ml kg<sup>-1</sup> h<sup>-1</sup> during the preparation phase and 7 ml kg<sup>-1</sup> h<sup>-1</sup> for the rest of the protocol. Once anaesthetised, the right internal jugular vein was cannulated with a pulmonary artery catheter used for continuous pulmonary artery pressure, intermittent thermodilution cardiac output, and core temperature monitoring.

### Data collection and processing

Cardiorespiratory variables, including peripheral oxyhaemoglobin saturation (SpO<sub>2</sub>), ECG, invasive arterial BP

(AS/3 Multi-Parameter Patient Monitor, Datex-Ohmeda, Madison, WI, USA), airway gas composition, flow, and pressure (Capnomac Ultima™; Datex-Ohmeda) were continuously monitored and acquired as analogue signals throughout the protocol. Analogue data were converted using PowerLab (ADInstruments, Dunedin, New Zealand) and displayed/recorded with LabChart version 8.1.5 (ADInstruments). Physiological data were processed using R version 3.5.1 (R Core Team (2017), Vienna, Austria).<sup>23</sup>

### Inspired sinewave technique

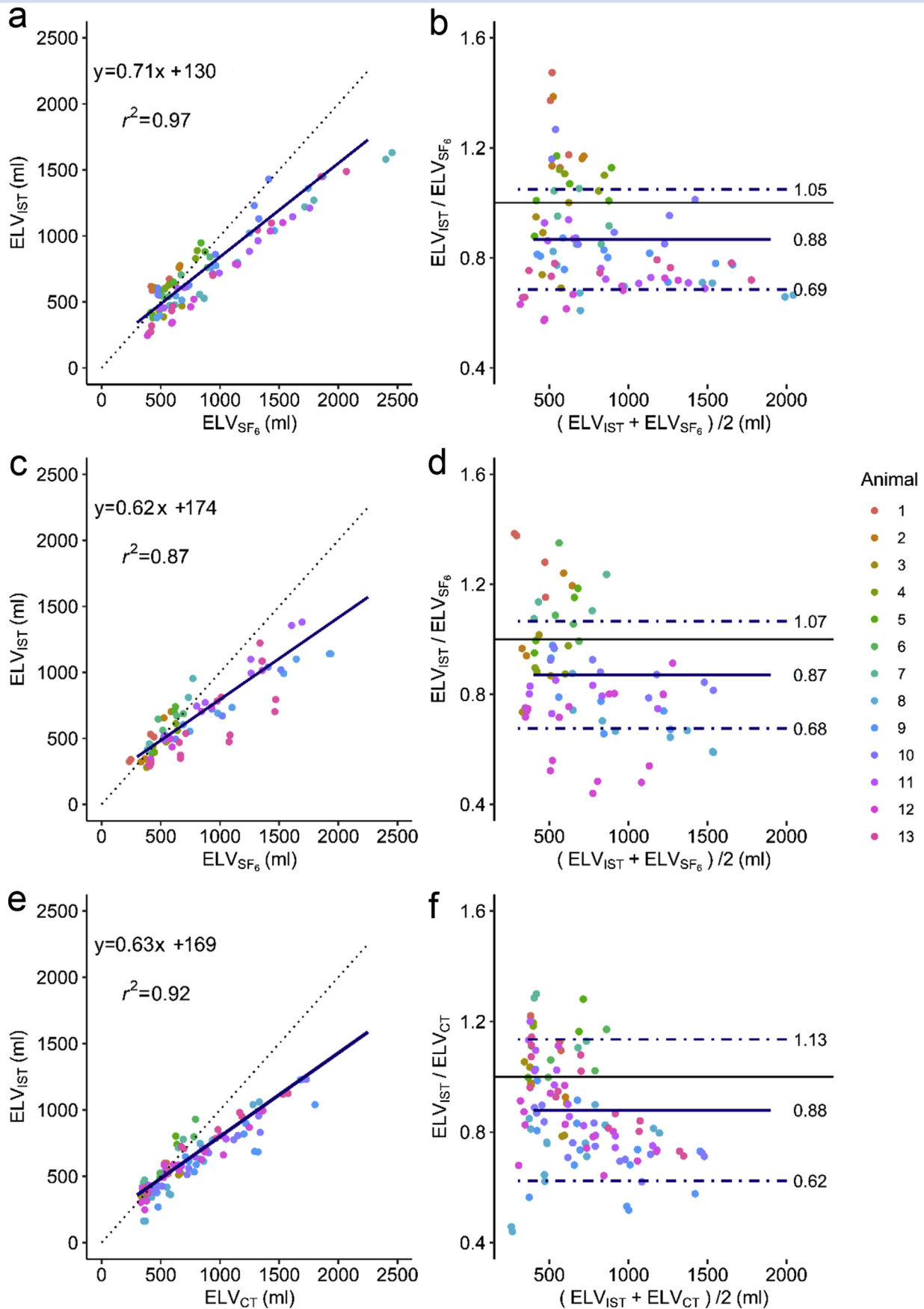
A mainstream infrared N<sub>2</sub>O and CO<sub>2</sub> sensor (IRMA, Danderyd, Thor Laboratories, Budapest Sweden) and an ultrasonic flowmeter (VenThor 22/2A; Thor Laboratories, Budapest, Hungary) were placed in the breathing circuit between a patient-end heat-moisture exchange filter (Intersurgical, Wokingham, UK) and the ventilator tubing. At the start of each inspiration, a set volume of N<sub>2</sub>O was injected into the inspired gas by a mass flow controller (Alicat Scientific, Tucson, AZ, USA). The volume of N<sub>2</sub>O injected was proportional to the inspiratory flow and oscillated sinusoidally over consecutive breaths around a set mean concentration of 5%, with an amplitude of 4% and a period of 180 s for a duration of 270 s. The test duration of 270 s was the maximum duration that would allow repetition of each test within the permitted time frame of the protocol. By measuring the expired N<sub>2</sub>O concentration in each consecutive breath, a set of simultaneous equations can be solved to provide estimates of ELV. Further technical details of IST are described elsewhere.<sup>15–17,24</sup>

### SF<sub>6</sub> wash in/washout

The use of SF<sub>6</sub> as a tracer gas for wash-in/washout measurement of lung volume is detailed elsewhere.<sup>10</sup> The apparatus was attached between the tracheal tube and the D-lite™ spirometer attachment (GE Healthcare, Chicago, IL, USA).

**Table 2** Descriptive statistics for comparisons of absolute effective lung volume (ELV) and changes in ELV ( $\Delta$ ELV) made in both the uninjured lung and the acute respiratory distress syndrome (ARDS) model at each PEEP level. Mean (standard deviation) volumes are shown in millilitres. n, number of observations (incomplete data sets have been excluded from the analysis; these account for 4% of total possible paired measurements). ELV<sub>CT</sub>, CT measured absolute volume; ELV<sub>IST</sub>, inspired sinewave technique (IST) measured absolute volume; ELV<sub>SF6</sub>, SF<sub>6</sub> measured absolute volume; P, probability from either two-way analysis of variance or Kruskal–Wallis that mean measurements at each PEEP level are from different samples;  $\Delta$ ELV<sub>CT</sub>, CT measured change in lung volume;  $\Delta$ ELV<sub>SF6</sub>, SF<sub>6</sub> measured change in lung volume.

| PEEP<br>(cm H <sub>2</sub> O) | Uninjured |                             |                             |         | ARDS model |                             |                             |         |    |                             |                            |         |
|-------------------------------|-----------|-----------------------------|-----------------------------|---------|------------|-----------------------------|-----------------------------|---------|----|-----------------------------|----------------------------|---------|
|                               | n         | ELV <sub>IST</sub>          | ELV <sub>SF6</sub>          | P-value | n          | ELV <sub>IST</sub>          | ELV <sub>SF6</sub>          | P-value | n  | ELV <sub>IST</sub>          | ELV <sub>CT</sub>          | P-value |
| 0                             | 17        | 422 (106)                   | 477 (66)                    | 0.35    | —          | —                           | —                           | —       | —  | —                           | —                          | —       |
| 5                             | 24        | 548 (99)                    | 607 (119)                   | 0.31    | 25         | 415 (108)                   | 444 (113)                   | 0.84    | 38 | 381 (76)                    | 394 (49)                   | 0.86    |
| 10                            | 22        | 734 (132)                   | 837 (169)                   | 0.14    | 26         | 601 (149)                   | 657 (157)                   | 0.26    | 36 | 598 (124)                   | 654 (99)                   | 0.14    |
| 15                            | 11        | 1022 (159)                  | 1377 (213)                  | 0.002   | 12         | 801 (207)                   | 1132 (249)                  | <0.0001 | 24 | 771 (107)                   | 1051 (177)                 | <0.0001 |
| 20                            | 12        | 1342 (194)                  | 1785 (373)                  | 0.01    | 12         | 1081 (197)                  | 1535 (214)                  | <0.0001 | 12 | 1077 (113)                  | 1493 (199)                 | <0.0001 |
|                               | n         | $\Delta$ ELV <sub>IST</sub> | $\Delta$ ELV <sub>SF6</sub> | P-value | n          | $\Delta$ ELV <sub>IST</sub> | $\Delta$ ELV <sub>SF6</sub> | P-value | n  | $\Delta$ ELV <sub>IST</sub> | $\Delta$ ELV <sub>CT</sub> | P-value |
| 0 to >5                       | 17        | 118 (60)                    | 180 (57)                    | 0.02    | —          | —                           | —                           | —       | —  | —                           | —                          | —       |
| 5 to >10                      | 24        | 190 (87)                    | 240 (71)                    | 0.13    | 26         | 191 (127)                   | 216 (91)                    | 0.81    | 24 | 209 (105)                   | 245 (58)                   | 0.60    |
| 10 to >15                     | 11        | 313 (90)                    | 423 (111)                   | 0.07    | 12         | 252 (73)                    | 399 (91)                    | 0.0008  | 12 | 196 (77)                    | 371 (90)                   | 0.0002  |
| 15 to >20                     | 12        | 312 (92)                    | 412 (233)                   | 0.56    | 12         | 281 (102)                   | 403 (70)                    | 0.008   | 12 | 370 (88)                    | 500 (75)                   | 0.005   |
| 20 to >15                     | —         | —                           | —                           | —       | —          | —                           | —                           | —       | 12 | -243 (92)                   | -383 (100)                 | 0.01    |
| 15 to >10                     | —         | —                           | —                           | —       | —          | —                           | —                           | —       | 12 | -233 (69)                   | -422 (67)                  | <0.0001 |
| 10 to >5                      | —         | —                           | —                           | —       | —          | —                           | —                           | —       | 12 | -242 (51)                   | -287 (64)                  | 0.37    |



### CT image acquisition and analysis

A Somatom Definition Flash (Siemens, Munich, Germany) was used to acquire images as a series of transverse sections with a reconstituted voxel size of  $0.5 \times 0.5 \times 5$  mm. Whole-lung volume scans were conducted during a 20 s end-expiratory pause without ventilator disconnection. Scans were taken using a tube voltage of 80 kV, 364 mA current, and  $64 \times 60$  mm collimation. Reconstituted whole-lung scans were segmented using 3D Slicer version 4.10.2<sup>25</sup> (<https://www.slicer.org/>). The mediastinum, diaphragm, inferior vena cava, and hilar vessels were not included in segmentation. Exclusion of intrapulmonary vessels within regions of increased voxel density was not possible, as they were not distinguishable from lung tissue, and these, along with the conducting airways up to the level of the clavicles, were included in the analysis. The aerated volume of each whole-lung scan was calculated from the Hounsfield unit (HU) density of each voxel according to the formula:<sup>26</sup>

$$\text{Aerated volume} = \frac{- \text{mean CT density (HU)}}{1000} \times \text{segmented volume}$$

### ARDS model

Lung injury was induced with a technique modified from Lachmann and colleagues.<sup>27</sup> Following preoxygenation, the ventilator was disconnected and the lungs lavaged by instillation of 0.9 % saline solution (at 37°C) via the tracheal tube. After 30 s, the saline was drained out of the lungs and ventilation recommenced. This process was repeated until a  $\text{PaO}_2:\text{FIO}_2$  ratio of less than 300 mm Hg was achieved.

### Study protocol

Throughout all phases of the protocol, the animals were positioned in dorsal recumbency;  $\text{FIO}_2$  was titrated to  $\text{PaO}_2 > 10$  kPa; and the animals were mechanically ventilated with VCV,  $V_T$  10 ml  $\text{kg}^{-1}$ , and I:E 1:2. The ventilatory frequency was adjusted to 15–20 bpm to maintain  $\text{EtCO}_2 < 8$  kPa. In all cases, measurements were taken after 2 min of ventilation at the studied PEEP level, and the tracheal tube was clamped during airway disconnection (e.g. to change equipment for measuring  $\text{ELV}_{\text{IST}}$  to  $\text{ELV}_{\text{SF}_6}$ ). [Supplementary Figure S1](#) shows a summary timeline of each experiment.

### Comparison between $\text{ELV}_{\text{IST}}$ and $\text{ELV}_{\text{SF}_6}$ pre- and post-injury

Measurements of ELV were taken with IST ( $\text{ELV}_{\text{IST}}$ ) and  $\text{SF}_6$  wash in/washout ( $\text{ELV}_{\text{SF}_6}$ ). Two sets of paired measurements were taken at each PEEP level studied. Measurements were taken first with IST, and then with  $\text{SF}_6$ . After completion of experiments in the uninjured model, lung injury was induced as described previously, and a further two paired

measurements of  $\text{ELV}_{\text{IST}}$  and  $\text{ELV}_{\text{SF}_6}$  were repeated at each PEEP level. In all 13 animals, the studied PEEP levels were 0, 5, and 10 cm  $\text{H}_2\text{O}$ . In six of these animals, PEEP levels of 15 and 20 cm  $\text{H}_2\text{O}$  were additionally included. In all comparisons of  $\text{ELV}_{\text{IST}}$  and  $\text{ELV}_{\text{SF}_6}$ , PEEP was incrementally increased from low to high. The protocol comparing  $\text{ELV}_{\text{IST}}$  and  $\text{ELV}_{\text{SF}_6}$  was the same pre- and post-saline lavage, except that 0 cm  $\text{H}_2\text{O}$  PEEP was not studied post-injury because of the risk that this would not be tolerated.

### Comparison between $\text{ELV}_{\text{IST}}$ and $\text{ELV}_{\text{CT}}$ after lung injury

Upon completion of the  $\text{ELV}_{\text{IST}}$  vs  $\text{ELV}_{\text{SF}_6}$  comparisons, the animals were transferred to the CT scanner. Two paired measurements of  $\text{ELV}_{\text{IST}}$  and ELV estimated from CT ( $\text{ELV}_{\text{CT}}$ ) were made at each PEEP level. In all 13 animals, the PEEP levels studied were 5 and 10 cm  $\text{H}_2\text{O}$ . In six of these animals, PEEP was titrated from 5 cm  $\text{H}_2\text{O}$  up to 20 cm  $\text{H}_2\text{O}$ , and then back down again. For the reason stated previously, zero PEEP was not studied post-injury. Upon completion of the study protocol, the anaesthetised pigs were euthanised with potassium chloride.

### Statistical analyses

Paired measurements of  $\text{ELV}_{\text{IST}}$ ,  $\text{ELV}_{\text{SF}_6}$ , and  $\text{ELV}_{\text{CT}}$  at each PEEP level were tested for normality using D'Agostino–Pearson's test and QQ plots. Datasets were compared with a repeated measures, two-way analysis of variance (ANOVA) with Sidak multiple comparison test.  $\Delta\text{ELV}$  was calculated by subtracting one absolute ELV from its value at the preceding PEEP level. The linear relationship between measurements was tested using linear mixed effects modelling with variation caused by different animals considered a random effect. Conditional  $r^2$  values based on the entire model are reported.<sup>28</sup> The agreement in measurements between techniques was assessed with Bland–Altman analysis corrected for multiple comparisons using a single-factor ANOVA with individual animal as the factor.<sup>29–31</sup> Non-normally distributed data were transformed (by using a ratio of measurements) to conform to the assumption of normality, and 95% limits of agreement were calculated as  $1.96 \text{ SD}$  from the mean bias. Measured changes in lung volume were compared using four quadrant plots with direction of change concordance and polar plots.<sup>32</sup> For polar plot analysis of trends, adequate limits of agreement are assumed to be within  $30^\circ$  of the horizontal. Analyses were carried out using R version 3.5.1 (R Core Development Team, Vienna, Austria),<sup>23</sup> GraphPad Prism version 8.1.2 (GraphPad Software, La Jolla, CA, USA; <https://www.graphpad.com/>), and SigmaPlot version 14.0 (Systat Software, San Jose, CA, USA).

### Results

A total of  $n=271$  paired ELV measurements in 13 pigs at five different PEEP levels were analysed. [Figure 1](#) shows that the

**Fig 2.** Scatter and Bland–Altman plots for absolute volume measurements ( $\text{ELV}_{\text{IST}}$ ,  $\text{ELV}_{\text{SF}_6}$ , and  $\text{ELV}_{\text{CT}}$ ). (a, b) Measurements from the uninjured lung. (c–f) Experiments conducted in the acute respiratory distress syndrome model. In the left column, scatterplots show the results of mixed effects linear models, where the solid line represents the reported equation. In the right column, solid lines in the Bland–Altman plots represent the mean bias, and the dashed lines show the upper and lower limits of agreement ( $\pm 1.96$  standard deviation). In all plots, individual points represent a paired set of measurements, and different colours represent different animals.

protocolised changes in PEEP induced changes in ELV, and that these changes were tracked by IST, SF<sub>6</sub>, and CT. Figure 1 and Table 2 show the comparisons of paired ELV and  $\Delta$ ELV measurements at each PEEP level. Statistical analyses suggested that ELV<sub>IST</sub> at 0, 5, and 10 cm H<sub>2</sub>O PEEP was not different from ELV<sub>SF6</sub> or ELV<sub>CT</sub> in both the uninjured lung and ARDS model. At 15 and 20 cm H<sub>2</sub>O PEEP, the measured

ELV<sub>IST</sub> was lower than ELV<sub>SF6</sub> and ELV<sub>CT</sub> in all comparisons (Table 2).

### Repeatability of ELV<sub>IST</sub> measurements

The mean coefficient of variation for ELV<sub>IST</sub> for each subject at each PEEP level was <5% in both the uninjured lung and the

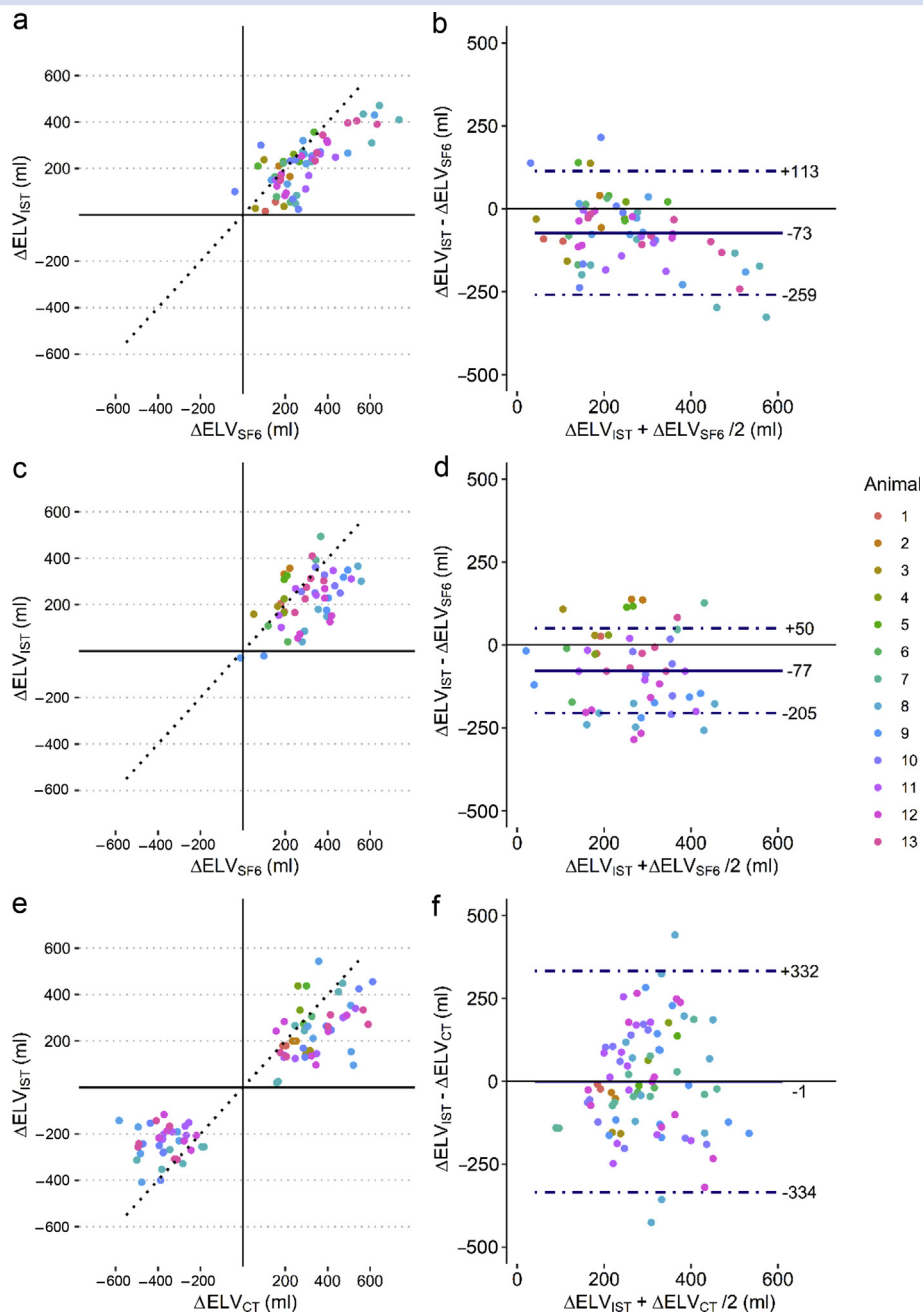


**Fig 3.** Scatter and Bland–Altman plots for changes in volume ( $\Delta$ ELV<sub>IST</sub>,  $\Delta$ ELV<sub>SF6</sub>, and  $\Delta$ ELV<sub>CT</sub>). (a, b) Measurements from the uninjured lung. (c–f) Experiments conducted in the ARDS model. In the left column, scatterplots show changes in volume. In the right column, solid lines in the Bland–Altman plots represent the mean bias, and the dashed lines show the upper and lower limits of agreement ( $\pm 1.96$  standard deviation). In all plots, individual points represent a paired set of measurements, and different colours represent different animals.

ARDS model; 90% of coefficients of variation for replicate measurements were <10%.

### Comparison between $ELV_{IST}$ , $ELV_{SF_6}$ , and $ELV_{CT}$

Figure 2a, c, and e show scatterplots and linear mixed effects regression for each of the comparisons. There was a robust linear relationship between  $ELV_{IST}$  and  $ELV_{SF_6}$  in both the uninjured lung ( $r^2=0.97$ ) and the ARDS model ( $r^2=0.87$ ). Similarly, we found a strong correlation between  $ELV_{IST}$  and  $ELV_{CT}$  in the ARDS model ( $r^2=0.92$ ).

### Agreement between $ELV_{IST}$ , $ELV_{SF_6}$ , and $ELV_{CT}$

Figure 2b, d, and f show that in each comparison,  $ELV_{IST}$  has a mean bias of 12–13% less than the reference technique in both the uninjured lung and the ARDS model.  $ELV_{IST}$  has limits of agreement with  $ELV_{SF_6}$  of  $\pm 17\%$  in the uninjured lung and  $\pm 20\%$  in the ARDS model. The limits of agreement between  $ELV_{IST}$  and  $ELV_{CT}$  were  $\pm 25\%$  in the ARDS model.

### Correlation between $\Delta ELV_{IST}$ , $\Delta ELV_{SF_6}$ , and $\Delta ELV_{CT}$

Figure 3a, c, and e show four quadrant plots demonstrating the relationship of  $\Delta ELV_{IST}$  with  $\Delta ELV_{SF_6}$  and  $\Delta ELV_{CT}$ . The linear relationship between  $\Delta ELV_{IST}$  and  $\Delta ELV_{SF_6}$  in the uninjured lung yielded an  $r^2=0.58$ , and  $r^2=0.83$  in the ARDS model. The linear relationship between  $\Delta ELV_{IST}$  and  $\Delta ELV_{CT}$  in the ARDS model had an  $r^2=0.16$ .

### Agreement between $\Delta ELV_{IST}$ , $\Delta ELV_{SF_6}$ , and $\Delta ELV_{CT}$

Direction of change concordance showed that  $\Delta ELV_{IST}$  has a concordance rate of 98–100% with  $ELV_{SF_6}$  and  $ELV_{CT}$ . This is reflected in Figure 3a, c, and e, where 98–100% of data are in the top right and bottom left quadrants of each four-quadrant plot. Figure 3b, d, and f show the Bland–Altman plots with a

mean bias (limits of agreement) of  $-73 (\pm 186)$  ml for  $\Delta ELV_{IST}$  vs  $\Delta ELV_{SF_6}$  in the uninjured lung,  $-77 (\pm 128)$  ml for  $\Delta ELV_{IST}$  vs  $\Delta ELV_{SF_6}$  in the ARDS model, and  $-1 (\pm 333)$  ml for  $\Delta ELV_{IST}$  vs  $\Delta ELV_{CT}$  in the ARDS model. Figure 4 demonstrates the polar agreement in paired measurements. The mean angular bias ranged from 8 to 11°, and radial limits of agreement from  $\pm 30$  to 37°.

## Discussion

This study presents the ability of IST to measure absolute ELV and changes in ELV, compared with the ‘gold standard’ techniques of  $SF_6$  wash in/washout ( $ELV_{SF_6}$ ) and CT ( $ELV_{CT}$ ) in uninjured lungs and in an ARDS model of lung injury. In both the uninjured lungs and a saline-lavage model of ARDS, IST can reliably measure the absolute ELV comparably with  $SF_6$  and CT, with acceptable measures of bias and limits of agreement. Additionally, when comparing PEEP-induced changes in lung volume, IST is >98% concordant with  $SF_6$  and CT.

IST measurements of absolute ELV are below those measured by  $SF_6$  and CT by 12–13% and do not fall within 5% of the reference method recommended by the European Respiratory Society/American Thoracic Society consensus statement.<sup>33</sup> These results are consistent with a previous study of IST, in which Bruce and colleagues<sup>17</sup> showed that IST underestimated functional residual capacity (FRC) by 32% (1080 ml) compared with body plethysmography in humans, where the mean FRC was 3.4 L. The underestimation was smaller in our study, with a mean bias of  $-12$  to  $-13\%$  ( $-129$  to  $-161$  ml), where the overall mean ELV was 809 ml. IST measures the volume of ventilated regions of the lung, and it is expected that IST will underestimate lung volume compared with CT, which estimates the entire thoracic gas volume. One reason for IST’s underestimation of ELV compared with  $SF_6$  may be that multi-breath washout

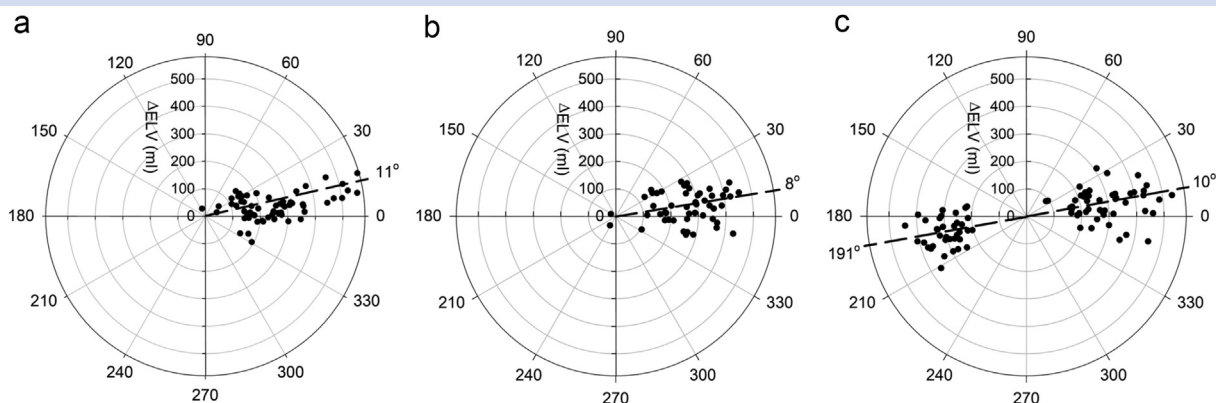


**Fig 4.** Polar plot analysis. The larger the mean  $\Delta ELV$ , the greater the distance between the point and the centre of the plot. The better the agreement between a pair of measurements, the closer the point lies to the horizontal ( $0^\circ$ ); 95% radial limits of agreement describe the angle within which 95% of the data lie. Concordance rate (%) describes the number of points that lie within the assumed limits of adequate agreement, set at  $\pm 30^\circ$ . (a) Comparison of  $\Delta ELV_{IST}$  vs  $\Delta ELV_{SF_6}$  in the uninjured lung. Mean angular bias= $11^\circ$ ; 95% radial limits of agreement= $\pm 35^\circ$ ; concordance= $91\%$ . (b) Comparison of  $\Delta ELV_{IST}$  vs  $\Delta ELV_{SF_6}$  in the acute respiratory distress syndrome (ARDS) model. Mean angular bias= $8^\circ$ ; 95% radial limits of agreement= $\pm 37^\circ$ ; concordance rate  $90\%$ . (c) Comparison of  $\Delta ELV_{IST}$  vs  $\Delta ELV_{CT}$  in the ARDS model. Mean angular bias= $10^\circ$  for positive changes in volume, and  $191^\circ$  for negative changes in volume; 95% radial limits of agreement= $\pm 30^\circ$ ; concordance rate= $95\%$ .

techniques recover tracer gas from the slowest compartments if the washout period is long enough, whereas for IST, the contribution of the slowest compartment is limited by the chosen period of the sinewave.

There is no previous study assessing the ability of IST to measure changes in lung volume. The linear relationship between  $\Delta ELV_{IST}$  and  $\Delta ELV_{SF_6}$  was stronger than for  $\Delta ELV_{CT}$ , and the limits of agreement were narrower for  $\Delta ELV_{SF_6}$  ( $\pm 186$  ml in the uninjured lung and  $\pm 128$  ml in the ARDS model) compared with  $\Delta ELV_{CT}$  ( $\pm 333$  ml). One proposed explanation for the narrower limits of agreement in the ARDS model compared with the uninjured model with  $SF_6$  was that the measured  $\Delta ELV$  was less in the ARDS model. Further analyses showed that the measured changes in volume (based on  $\Delta ELV_{SF_6}$ ) were no different in the uninjured and ARDS models (PEEP 5–10:  $P=0.11$ ; PEEP 10–15:  $P=0.59$ ; PEEP 15–20:  $P=0.91$ ). The repeatability of IST measurements of ELV in the same subject under the same conditions was within the reported international acceptable limits of coefficient of variation ( $<10\%$ )<sup>34</sup> and consistent with studies of IST in other circumstances.<sup>17</sup> IST has good repeatability and minimal bias compared with CT (mean bias =  $-1$  ml) when measuring changes in lung volume. This provides support for the use of IST to monitor trends in lung volume, where the change (or lack of) in volume after a change in ventilator setting is potentially of most interest to the bedside clinician.

The inspired sinewave technique offers several strengths, including commercial availability of component parts and its ease of use at the bedside. As IST does not rely on a fixed inspiratory flow, it can be used in spontaneously ventilating patients. The main limitations of our study are that the use of a porcine model does not directly translate to humans, and the use of saline lavage does not necessarily comprise all the features of human ARDS. However, saline lavage does result in reduction in lung volume, which is one reason for its choice in this study. In addition, in this protocol, not all PEEP levels were studied in all experiments. This was not feasible due to time restraints because the initial seven experiments including PEEP 0, 5, and 10 cm H<sub>2</sub>O were undertaken in parallel with data collection for another study, in keeping with the 3Rs principle.<sup>35</sup> Future development of IST could include assessing the feasibility of its use in mechanically ventilated human patients. IST development will enable the measurement of lung volumes when using volume-controlled and pressure-controlled ventilation modes in paralysed patients and in assisted mechanical ventilation, where less regular inspiratory flow patterns exist.

The inspired sinewave technique is a potentially translatable research tool and this study is the first to examine its use in mechanically ventilated lungs. Measuring the size of the ARDS baby lung would allow titration of  $\Delta P$  to the individual patient, either directly<sup>7</sup> or by scaling  $V_T$  to the size of the baby lung. This has the potential to reduce mortality in patients with ARDS. We have demonstrated that IST measured lung volumes and changes in volume reliably compared to the standard techniques of  $SF_6$  washin-washout and CT in a mechanically ventilated porcine model. Our results support further development of this technique and its translation to human medicine.

### Authors' contributions

Study design: DCC, FF, PAP  
Experimentation: DCC, JNC, MCT, PAP

Data analysis: DCC

Data interpretation: DCC, MCT, FF, JNC, ADF

Financial support: FF, PAP, AL, ADF

Writing manuscript: DCC

Critical revision: DCC, MCT, JNC, FF, AL, ADF

### Acknowledgements

The authors are grateful to Agneta Roneus, Kerstin M. Ahlgren, Maria Swålas, Mariette Andersson, Liselotte Pihl, and Monica Segelsjö for technical support; to OxSTaR, St Peter's College, and the Nuffield Division of Anaesthetics office for their ongoing support of DCC; and to Richard Bruce and Joao Batista-Borges for their helpful advice.

### Declarations of interest

ADF and PAP are named inventors on a patent application (EP3122249A1/US20170100043A1 [pending]) submitted by the University of Oxford, which may receive financial benefit when the technology is commercialised.

### Funding

National Institute for Health Research (II-LA-0214-20005 and NIHR200029) to PAP and ADF; Royal Academy of Engineering Enterprise Fellowship to PAP; Swedish Heart-Lung Foundation (20170531) to AL and GH; Swedish Research Council (K2015-99X-2273101-4) to AL and GH; Medical Research Council (MC\_PC\_17164) to FF; The Physiological Society (Formenti 2018) to FF.

### Appendix A. Supplementary data

Supplementary data to this article can be found online at <https://doi.org/10.1016/j.bja.2019.11.030>.

### References

- Bellani G, Laffey JG, Pham T, et al. Epidemiology, patterns of care, and mortality for patients with acute respiratory distress syndrome in intensive care units in 50 countries. *JAMA* 2016; 315: 788–800
- Acute Respiratory Distress Syndrome Network, Brower RG, Matthay MA, et al. Ventilation with lower tidal volumes as compared with traditional tidal volumes for acute lung injury and the acute respiratory distress syndrome. *N Engl J Med* 2000; 342: 1301–8
- Gattinoni L, Marini JJ, Pesenti A, Quintel M, Mancebo J, Brochard L. The “baby lung” became an adult. *Intensive Care Med* 2016; 42: 663–73
- Gattinoni L, Pesenti A. The concept of “baby lung”. *Intensive Care Med* 2005; 31: 776–84
- Amato MB, Meade MO, Slutsky AS, et al. Driving pressure and survival in the acute respiratory distress syndrome. *N Engl J Med* 2015; 372: 747–55
- Hubmayr RD, Kallet RH. Understanding pulmonary stress-strain relationships in severe ARDS and its implications for designing a safer approach to setting the ventilator. *Respir Care* 2018; 63: 219–26
- Grieco DL, Chen L, Dres M, Brochard L. Should we use driving pressure to set tidal volume? *Curr Opin Crit Care* 2017; 23: 38–44



8. Richard J-C, Pouzot C, Pinzón AM, et al. Reliability of the nitrogen washin-washout technique to assess end-expiratory lung volume at variable PEEP and tidal volumes. *Intensive Care Med Exp* 2014; 2: 10
9. Heinze H, Eichler W. Measurements of functional residual capacity during intensive care treatment: the technical aspects and its possible clinical applications. *Acta Anaesthesiol Scand* 2009; 53: 1121–30
10. Larsson A, Linnarsson D, Jonmarker C, Jonson B, Larsson H, Werner O. Measurement of lung volume by sulfur hexafluoride washout during spontaneous and controlled ventilation: further development of a method. *Anesthesiology* 1987; 67: 543–50
11. Di Marco F, Rota Sperti L, Milan B, et al. Measurement of functional residual capacity by helium dilution during partial support ventilation: in vitro accuracy and in vivo precision of the method. *Intensive Care Med* 2007; 33: 2109–15
12. Maisch S, Boehm SH, Weismann D, et al. Determination of functional residual capacity by oxygen washin-washout: a validation study. *Intensive Care Med* 2007; 33: 912–6
13. Patroniti N, Saini M, Zanella A, et al. Measurement of end-expiratory lung volume by oxygen washin-washout in controlled and assisted mechanically ventilated patients. *Intensive Care Med* 2008; 34: 2235–40
14. Zwart A, Seagrave RC, Dieren AV. Ventilation-perfusion ratio obtained by a noninvasive frequency response technique. *J Appl Physiol* 1976; 41: 419–24
15. Hahn CE. Oxygen respiratory gas analysis by sine-wave measurement: a theoretical model. *J Appl Physiol* 1996; 81: 985–97
16. Hahn CE, Black AM, Barton SA, Scott I. Gas exchange in a three-compartment lung model analyzed by forcing sinusoids of N<sub>2</sub>O. *J Appl Physiol* 1993; 75: 1863–76
17. Bruce RM, Phan PA, Pacpaco E, Rahman NM, Farmery AD. The inspired sine-wave technique: a novel method to measure lung volume and ventilatory heterogeneity. *Exp Physiol* 2018; 103: 738–47
18. Phan PA, Zhang C, Geer D, Formenti F, Hahn CEW, Farmery AD. The inspired sinewave technique: a comparison study with body plethysmography in healthy volunteers. *IEEE J Transl Eng Health Med* 2017; 5: 2700209
19. Gattinoni L, Mascheroni D, Torresin A, et al. Morphological response to positive end expiratory pressure in acute respiratory failure. Computerized tomography study. *Intensive Care Med* 1986; 12: 137–42
20. Gattinoni L, Pesenti A, Avalli L, Rossi F, Bombino M. Pressure-volume curve of total respiratory system in acute respiratory failure. Computed tomographic scan study. *Am Rev Respir Dis* 1987; 136: 730–6
21. Kilkeny C, Browne WJ, Cuthill IC, Emerson M, Altman DG. Improving bioscience research reporting: the ARRIVE guidelines for reporting animal research. *PLoS Biol* 2010; 8, e1000412
22. Crockett DC, Cronin JN, Bommakanti N, et al. Tidal changes in PaO<sub>2</sub> and their relationship to cyclical lung recruitment/derecruitment in a porcine lung injury model. *Br J Anaesth* 2019; 122: 277–85
23. R Development Core Team R. *A language and environment for statistical computing*. Vienna, Austria: R Foundation for Statistical Computing; 2017
24. Phan PA, Zhang C, Geer D, Hahn C, Farmery A. Inspired sinewave technique: a novel technology to measure cardiopulmonary function. In: Toi VV, Lien Phuong TH, editors. *5th international conference on biomedical engineering in vietnam*. Cham: Springer; 2015. p. 83–6
25. Fedorov A, Beichel R, Kalpathy-Cramer J, et al. 3D slicer as an image computing platform for the quantitative imaging network. *Magn Reson Imaging* 2012; 30: 1323–41
26. Chiumello D, Cressoni M, Chierichetti M, et al. Nitrogen washout/washin, helium dilution and computed tomography in the assessment of end expiratory lung volume. *Crit Care* 2008; 12: R150
27. Lachmann B, Robertson B, Vogel J. In vivo lung lavage as an experimental model of the respiratory distress syndrome. *Acta Anaesthesiol Scand* 1980; 24: 231–6
28. Nakagawa S, Schielzeth H, O'Hara RB. A general and simple method for obtaining R<sup>2</sup> from generalized linear mixed-effects models. *Methods Ecol Evol* 2013; 4: 133–42
29. Bland JM, Altman DG. Statistical methods for assessing agreement between two methods of clinical measurement. *Lancet* 1986; 1: 307–10
30. Bland JM, Altman DG. Measuring agreement in method comparison studies. *Stat Methods Med Res* 1999; 8: 135–60
31. Bland JM, Altman DG. Agreement between methods of measurement with multiple observations per individual. *J Biopharm Stat* 2007; 17: 571–82
32. Critchley LA, Lee A, Ho AM. A critical review of the ability of continuous cardiac output monitors to measure trends in cardiac output. *Anesth Analg* 2010; 111: 1180–92
33. Robinson PD, Latzin P, Verbanck S, et al. Consensus statement for inert gas washout measurement using multiple- and single-breath tests. *Eur Respir J* 2013; 41: 507–22
34. Wanger J, Clausen JL, Coates A, et al. Standardisation of the measurement of lung volumes. *Eur Respir J* 2005; 26: 511–22
35. Russell WMS, Burch RL, Hume CW. *The principles of humane experimental technique*. London: Methuen; 1959